

Scaling behavior of an Anderson impurity close to the Mott-Anderson transition

M. C. O. Aguiar,¹ V. Dobrosavljević,² E. Abrahams,¹ and G. Kotliar¹

¹Center for Materials Theory, Serin Physics Laboratory,

Rutgers University, 136 Frelinghuysen Road, Piscataway, New Jersey 08854

²Department of Physics and National High Magnetic Field Laboratory, Florida State University, Tallahassee, FL 32306

The scaling behavior of Anderson impurity models each of which with a different site energy ε_i is examined close to the Mott-Anderson transition. Depending on its impurity energy ε_i , in the critical regime a site turns into a local magnetic moment, as indicated by a vanishing quasiparticle weight $Z \rightarrow 0$, or remains nearly doubly occupied or nearly empty, corresponding to $Z \rightarrow 1$. In this paper, we present the scaling behavior of Z as a function of the on-site energy ε_i and the distance t to the transition, and interpret our result in terms of an appropriate beta function $\beta(Z)$.

PACS numbers: 71.27.+a, 72.15.Rn, 71.30.+h

I. INTRODUCTION

The Mott¹ and the Anderson² routes to localization have long been recognized as two of the basic processes that can drive the metal-insulator transition. Theories separately describing each of these mechanisms were discussed long ago. According to the scaling theory of localization,³ for example, any amount of disorder drives a system with dimension smaller or equal to two to an insulator phase. However, this result was derived considering Anderson localization effects due to disorder, in the absence of electron-electron interaction.

Several years after the scaling theory of localization,³ the groundbreaking work of Finkelstein⁴ suggested for the first time the existence of a possible metallic phase in two dimensions for disordered correlated systems. In Ref. 4, the effects of correlation and disorder were included by a perturbative renormalization group approach based on the Fermi liquid theory. These results are valid in the diffusive regime. Behavior in the ballistic regime was later considered by Gold and Dolgoplov,⁵ by Das Sarma and Hwang,⁶ and by Zala *et al.*⁷ Most recently, Punnoose and Finkelstein⁸ have extended the latter's earlier work⁴ to give a description of metallic behavior in two-dimensional semiconductor structures. However, all these works focus on corrections to the Fermi liquid theory and as such are appropriate in the weak coupling regime.⁹ Such perturbative approaches cannot properly describe strong correlation effects, such as the approach to the Mott transition, or the associated transmutation of conduction electrons into local magnetic moments. These processes are of key importance in many materials of recent interest, ranging from doped transition metal oxides and doped semiconductors to organic Mott systems.

To describe systems in which both the correlations and the disorder effects are strong, complementary methods are required. This is the situation we examine in the present paper, where we focus on extensions of the dynamical mean field theory (DMFT).^{10,11,12} These extensions are local mean field approaches, which certainly cannot provide a proper description of fluctuation effects in low dimensions. Nevertheless, they can be considered

as the simplest approaches incorporating both the Mott and the Anderson routes to localization. Even simple estimates indicate that in many systems both of these processes play comparable roles, and as a result they cannot be considered separately. Addressing the behavior in this nonperturbative regime is the main subject of this work.

In the following, we first briefly review the principal physical ideas on the interplay of correlations and disorder, as already presented in the early works of Mott.¹ We then discuss how this physical behavior is naturally described by the extended DMFT approaches which are the main subject of this paper.^{11,12}

A. Effects of disorder: early ideas

A first glimpse of the basic effect of disorder on the Mott transition was outlined by Mott,¹ who pointed out that important consequences of disorder can be seen even

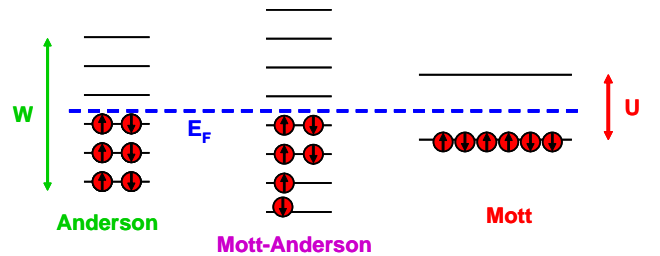


FIG. 1: (Color online) Energy level occupation in the strongly localized (atomic) limit for an Anderson (left), a Mott (right), and a Mott-Anderson (center) insulator. In a Mott-Anderson insulator, the disorder strength W is comparable to the Coulomb repulsion U , and a two-fluid behavior emerges. Here, a fraction of localized states are doubly occupied or empty as in an Anderson insulator. Coexisting with those, other states remain singly occupied forming local magnetic moments, as in a Mott insulator. Note that the spins of the local moments may be randomly oriented indicating the absence of magnetic ordering. The chemical potential is represented by the dashed line.

when the correlations are so strong that the system is in the strongly localized (atomic) limit. In the absence of disorder, each site has two energy levels, $\varepsilon_0 = 0$ and $\varepsilon_1 = U$, where U is the on-site interaction potential. If the system is half-filled, then each site is singly occupied; the levels ε_1 remain empty. We have one local magnetic moment at each site, and a gap equal to U to charge excitations (as schematically represented in Fig. 1 on the right).

When disorder is added, each of these energy levels is shifted by a randomly fluctuating site energy $-W/2 < \varepsilon_i < W/2$. The situation remains unchanged for $W < U$, as all the levels $\varepsilon'_1(i) = U + \varepsilon_i$ remain empty (for half-filling the chemical potential is $\mu = E_F = U/2$). For larger disorder, those sites with $\varepsilon_i > U/2$ have the level $\varepsilon'_0(i) = 0 + \varepsilon_i > \mu$ and are empty. Similarly, those sites with $\varepsilon_i < -U/2$ have the excited level $\varepsilon'_1(i) = U + \varepsilon_i < \mu$ and are doubly occupied. Thus for $W > U$ a fraction of the sites are either doubly occupied or empty. The Mott gap is now closed, although a fraction of the sites still remain as localized magnetic moments. We can describe this state as an inhomogeneous mixture of a Mott and an Anderson insulator (as shown in the center of Fig. 1). However, the empty and doubly occupied sites have succeeded to completely fill the gap in the average single particle density-of-states (DOS).

This physical picture of Mott is very transparent and intuitive. The nontrivial question is how the strongly localized (atomic) limit is approached as one crosses the metal-insulator transition from the metallic side. To address this question one needs a more detailed theory for the metal-insulator transition region, which was not available when the questions posed by Mott and Anderson were put forward.

B. DMFT description of the Mott-Anderson transition

The early ideas of Mott have been elaborated and put on a considerably firmer ground by the development of DMFT approaches. Here,¹⁰ the many-body problem is reduced to focusing on a single site in the lattice and solving for the dynamics of an electron trying to delocalize by escaping into its environment. The solution of such an Anderson impurity problem depends very strongly on the spectrum of electronic states $\Delta(\omega)$ describing the environment, a quantity determined by an appropriate self-consistency condition defined by the lattice model in question.¹⁰ In the presence of disorder, we have an *ensemble* of single-impurity problems and the self-consistency condition involves the algebraic average of local quantities over the ensemble. This theory provides the currently best available description of the Mott metal-insulator transition, but standard DMFT fails to incorporate Anderson localization effects.

Localization effects within DMFT: *statDMFT*

To overcome this difficulty, in a recent work¹¹ DMFT was extended by allowing for spatial fluctuations of the cavity spectrum, now given by $\Delta_i(\omega)$ (note the index i). This led to the so-called *statDMFT* approach, which followed the original method of Anderson.² Here, one takes the local point of view, but looks at the typical values of the quantities, that is, to their most probable values. In particular, one can examine the typical escape rate, which is given by the typical DOS available to escape from a given lattice site. These accessible levels are typically found away from the Fermi energy, reducing the relevant spectral weight “seen” by the local electron. The *statDMFT* approach is intuitively appealing and physically well-justified; its limitation is the extensive numerical work required to solve the associated stochastic equations.

Typical Medium Theory

An alternative and much simpler approach was recently provided by the typical medium theory (TMT),¹² in which the local spectrum of the effective medium is replaced by its geometric (typical) average. This approach proved able to reproduce many expected features of the Anderson localization transition for dimension larger than 2. It can be viewed as the conceptually simplest local picture of the Anderson localization. In this approximation, the spectral weight of the cavity is reduced as the Anderson transition is approached.

Even before doing any calculations, one may anticipate that such an elementary manifestation of incipient localization should dramatically affect the correlation effects when the electron-electron interaction is turned on. Very recent work by Byczuk *et al.*¹³ followed a TMT approach and confirmed that (in contrast to standard DMFT) it provides a consistent description of both Mott and Anderson transition in the limiting cases and also of the Mott-Anderson transition when both interaction and disorder are present. A phase diagram obtained by employing a numerical renormalization group impurity solver was presented. However, a more detailed understanding of the physical behavior in the critical regime, such as possible scaling properties and power-law behavior, was not elucidated.

To have a better understanding of what is going on, we use a “4-boson” impurity solver (in the following call it SB4) of Kotliar and Ruckenstein¹⁴ to examine the critical behavior at the Mott-Anderson transition. Before having a complete description of this critical behavior, it is important to first understand in detail the critical behavior of the local impurity models, and this is what we concentrate on in this paper.

C. Critical behavior of the impurity models

It is clear from the above discussion of the atomic limit, as well as from the previous *stat*DMFT results,¹¹ that for $W > U$ the Mott-Anderson transition has a qualitatively different character than either the pure Mott or Anderson transitions. One has to deal with a two-fluid situation, as a fraction of the electrons become local magnetic moments and the other fraction remains in magnetically inert configurations.

In this paper, we explore this two-fluid picture from the point of view of single-impurity problems with different on-site energies. Instead of addressing the structure of the self-consistent solution, we examine a simpler problem, where we use a simple model to describe the behavior of the cavity spectrum. More specifically, we look at the behavior of a collection of Anderson impurity models, defined by the local site energies ε_i as, guided by the TMT results,¹⁵ we reduce the spectral weight of the bath function. The latter is a measure of the distance t to the transition and we thus mimic the approach to it.

We find that when the distance t to the transition decreases, depending on the value of the impurity on-site energy ε_i , the quasiparticle weight Z_i goes either to 0 or 1. We explore in detail the scaling behavior of Z_i as a function of t and ε_i , which can be expressed in an elegant form using an appropriate β -function formulation, as described below. We anticipate that our detailed understanding of this scaling behavior will allow for an analytical solution of the critical behavior within the full self-consistent theory. This interesting direction is left for future work. Note, though, that the analysis presented in this paper describes properties of quantum impurities in a metallic host and is therefore relevant for that class of problem.

The paper is organized as follows. In section II, we present the single-impurity models we solved and the method used to do it. In section III, we discuss the β -function formulation valid for the problem in question. We finish by presenting our conclusions in section IV.

II. ANDERSON IMPURITY CLOSE TO AN INSULATING STATE

In DMFT language, a given site is seen as an Anderson impurity that has the freedom to dynamically choose between a singlet or a doublet (local moment) solution upon entering the insulator. The relevant impurity model is characterized by the on-site repulsion U , the on-site energy ε_i and the total spectral weight t of the cavity field (this is defined in terms of t below). The hamiltonian describing the problem is given by

$$H = \sum_{\vec{k}\sigma} \varepsilon_{\vec{k}\sigma} c_{\vec{k}\sigma}^\dagger c_{\vec{k}\sigma} + V \sum_{i\sigma} \left(c_{i\sigma}^\dagger f_\sigma + f_\sigma^\dagger c_{i\sigma} \right) + (\varepsilon_i - \mu) \sum_{\sigma} f_{\sigma}^\dagger f_{\sigma} + U f_{\uparrow}^\dagger f_{\uparrow} f_{\downarrow}^\dagger f_{\downarrow}, \quad (1)$$

where $c_{\vec{k}\sigma}$ and f_σ are annihilation operators of extended and localized electrons, respectively, and V and $\varepsilon_{\vec{k}}$ define the cavity field $\Delta(\omega_n) = V^2 \sum_{\vec{k}} [1/(\omega_n - \varepsilon_{\vec{k}})]$. Alternatively, the cavity function can be written in the spectral form

$$\Delta(\omega_n) = V^2 \int_{-\infty}^{\infty} d\omega \frac{\rho_{typ}(\omega)}{\omega_n - \omega}. \quad (2)$$

We used two different forms for $\rho_{typ}(\omega)$:

1. The typical DOS calculated self-consistently when approaching the Mott-Anderson transition.¹⁵ An

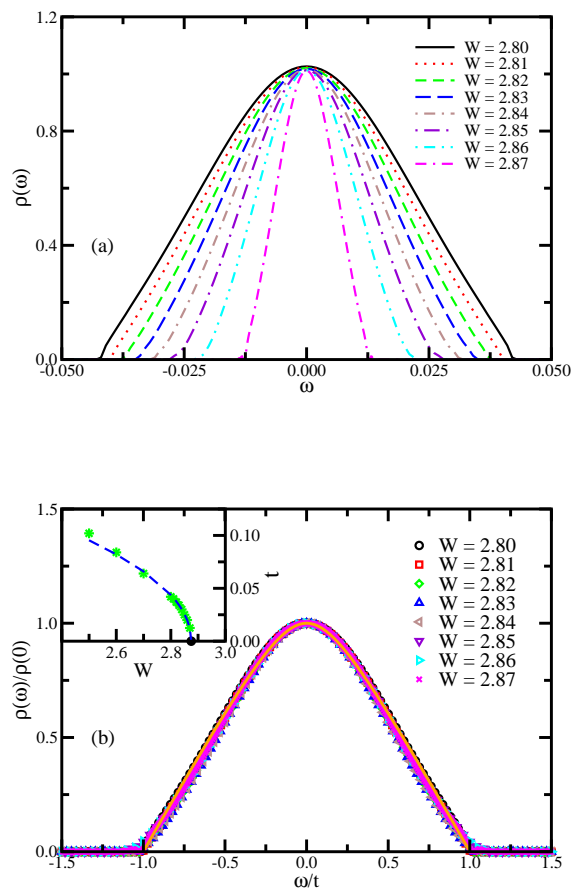


FIG. 2: (Color online) (a) Evolution of the typical DOS obtained for the disordered Hubbard model close to the Mott-Anderson transition, approached by fixing the interaction U and increasing the disorder W . The problem is solved using DMFT-TMT. The disorder is present in the on-site energy, which follows a uniform distribution of width W . The bare DOS is a semicircle of width $2D = 1$. (b) Scaling of the results in (a). The typical DOS for different W can be fit to a single function by scaling the frequency. The inset shows that the scaling parameter t decreases as the disorder increases and follows a powerlaw (the dashed line is a powerlaw fitting to the numerical data).

example can be seen in Fig. 2 for $U = 1.75$ and different values of the breadth of the disorder W . We find that, as the transition is approached, the spectrum retains the same shape, while mainly the total spectral weight, determined here by the spectrum width, decreases [see panel (a)].¹⁶ Besides, as shown in panel (b), the results can be scaled to a single function, with the scaling parameter t (inset) having a powerlaw dependence on W . Here t is a measure of the spectrum width.

2. A featureless model bath given by 1 for $-t/2 < \omega < t/2$ and zero otherwise, with $t \rightarrow 0$ at the transition.

As we shall see, the qualitative critical behaviors of the impurity models are not affected by the specific choice of the spectral function, as identical critical exponents are obtained for the two models. This is important, since a simple featureless model offers a considerable advantage for analytical work.

The impurity model of Eq. (1) was solved at zero temperature using the SB4 method,¹⁴ which provides a parametrization of the low-energy (quasiparticle) part of the local Green's function, given by

$$G_i(\omega_n) = \frac{Z_i}{i\omega_n - \tilde{\varepsilon}_i - Z_i\Delta(\omega_n)}, \quad (3)$$

where Z_i is the local quasiparticle weight and $\tilde{\varepsilon}_i$ is the renormalized site energy. The approach consists of determining the site-dependent parameters e_i , d_i and $\tilde{\varepsilon}_i$ by the following equations

$$-\frac{\partial Z_i}{\partial e_i} \frac{1}{\beta} \sum_{\omega_n} \Delta(\omega_n) G_i(\omega_n) = Z_i (\mu + \tilde{\varepsilon}_i - \varepsilon_i) e_i, \quad (4)$$

$$-\frac{\partial Z_i}{\partial d_i} \frac{1}{\beta} \sum_{\omega_n} \Delta(\omega_n) G_i(\omega_n) = Z_i (U - \mu - \tilde{\varepsilon}_i + \varepsilon_i) d_i, \quad (5)$$

$$\frac{1}{\beta} \sum_{\omega_n} G_i(\omega_n) = \frac{1}{2} Z_i (1 - e_i^2 + d_i^2), \quad (6)$$

where $Z_i = 2(e_i + d_i)^2 [1 - (e_i^2 + d_i^2)] / [1 - (e_i^2 - d_i^2)^2]$ in terms of e_i and d_i and $\mu = U/2$.

The results for the quasiparticle weight Z_i as a function of ε_i are shown in Fig. 3 for the flat bath function explained above. Almost identical results are found for the self consistent typical bath of Fig. 2. We shall examine the situation where the spectral weight t goes to zero, meaning that the system goes towards the Mott-Anderson transition.

Considering many single-impurity problems, we observe a two-fluid picture, just as in the limit earlier analyzed by Mott.¹ Indeed, these results correspond to the

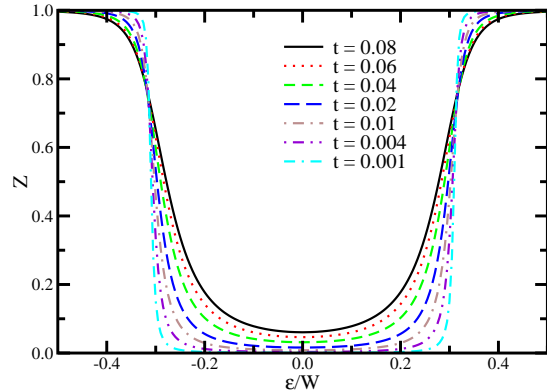


FIG. 3: (Color online) Quasiparticle weight Z as a function of the on-site energy ε for the single-impurity problems close to the Mott-Anderson transition. A flat bath (see text) was used. The transition is approached when the bath weight t decreases towards 0. The parameters used were $U = 1.75$ and $W = 2.8$.

same atomic limit discussed by Mott, since, although the hopping itself is still finite, the cavity field “seen” by the impurities goes to zero in the current case. One can either look at the results as a function of ε_i for different values of t , as presented in Fig. 3, or look at the same data plotted as a function of t for different values of ε_i , as shown in Fig. 4.

As in the atomic limit, the sites with $|\varepsilon_i| < U/2$

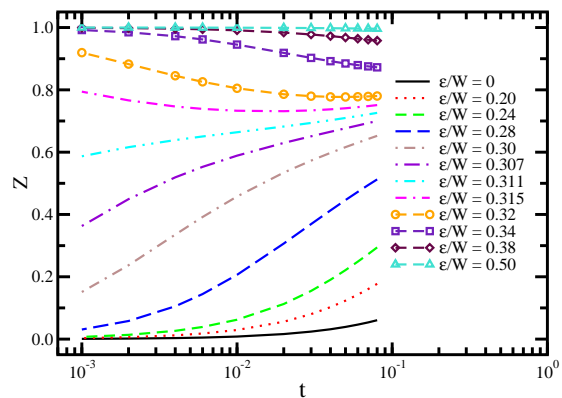


FIG. 4: (Color online) Same results as in Fig. 3 for the quasiparticle weight Z plotted in a different way: as a function of t for different values of ε/W (instead of as a function of ε/W for different values of t , as before). We present the results only for positive site energies, as a similar behavior holds for negative ones. Other parameters as in Fig. 3.

turn into local moments and have vanishing quasiparticle weight $Z_i \rightarrow 0$. The remaining sites show $Z_i \rightarrow 1$, as they are either doubly occupied, which corresponds to those with $\varepsilon_i < -U/2$, or empty, which is the case for those sites with $\varepsilon_i > U/2$. Consequently, as the transition is approached, the curves $Z(\varepsilon_i, t)$ “diverge” and approach either $Z = 0$ or $Z = 1$. These values of Z can thus be identified as two stable fixed points for the problem in question, as we discuss below.

Note that in Fig. 4 we restrict the results to positive energy values, as a similar behavior is observed for negative ε_i . In this case, there is precisely one value of the site energy $\varepsilon_i = \varepsilon^*$, for which $Z(\varepsilon^*, t) \rightarrow Z^*$. This corresponds to the value of ε_i below which Z “flows” to 0 and above which Z “flows” to 1. In other words, it corresponds to an unstable fixed point. Just as in the atomic limit, ε^* is equal to $U/2$ ($\varepsilon^*/W = 0.3125$ in Fig. 4, where $U = 1.75$ and $W = 2.8$).

Interestingly, the family of curves in Fig. 4 looks similar to those seen in some other examples of quantum critical phenomena. In fact, one can say that the crossover scale t plays the role of the reduced temperature, and the reduced site energy $\delta\varepsilon = (\varepsilon_i - \varepsilon^*)/\varepsilon^*$ that of the control parameter of the quantum critical point. As the site energy is tuned at $t = 0$, the impurity model undergoes a phase transition from a singlet to a doublet ground state. Quantum fluctuations associated with the metallic host introduce a cutoff and round this phase transition, which becomes sharp only in the $t \rightarrow 0$ limit. In the following, we develop a detailed scaling analysis of the $t = 0$, $\delta\varepsilon = 0$ fixed point based on our numerical and analytical results obtained from the SB4 impurity model solution.¹⁴

III. β -FUNCTION FORMULATION

Our numerical solutions provide evidence that as a function of t the “charge” $Z(t)$ “flows” away from the unstable “fixed point” Z^* , and towards either stable “fixed points” $Z = 0$ or $Z = 1$. The structure of these flows show power-law scaling as the scale $t \rightarrow 0$; this suggests that it should be possible to collapse the entire family of curves $Z(t, \delta\varepsilon)$ onto a single universal scaling function

$$Z(t, \delta\varepsilon) = f[t/t^*(\delta\varepsilon)], \quad (7)$$

where the crossover scale $t^*(\delta\varepsilon) = C^\pm |\delta\varepsilon|^\phi$ around the unstable fixed point. Remarkably, we have been able to scale the numerical data precisely in this fashion, see Fig. 5, and extract the form of $t^*(\delta\varepsilon)$. According to Fig. 6, $t^*(\delta\varepsilon)$ does vanish in a power law fashion at $\delta\varepsilon = 0$, with exponent $\phi = 2$ and the amplitudes C^\pm differ by a factor close to two for $Z \gtrless Z^*$.

As shown in Fig. 5, the scaling function $f(x)$ where $x = t/t^*(\delta\varepsilon)$ presents two branches: one for $\varepsilon_i < \varepsilon^*$ and other for $\varepsilon_i > \varepsilon^*$. We found that for $x \rightarrow 0$ both branches of $f(x)$ are linear in x [Fig. 7(a) and 7(b)], while for $x \gg 1$ they merge, i.e. $f(x) \rightarrow Z^* \pm A^\pm x^{-1/2}$ [Fig. 7(c)]. As can be seen in the first two panels, in the limit $t \rightarrow 0$,

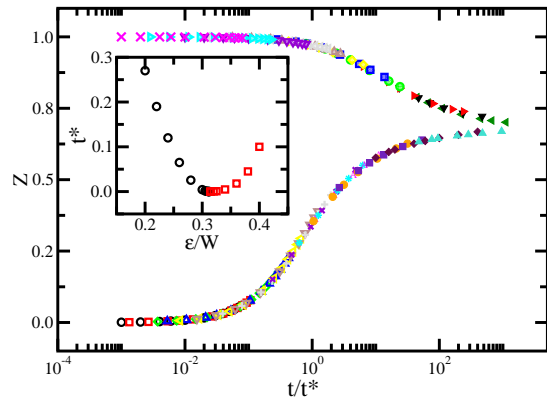


FIG. 5: (Color online) Quasiparticle weight Z as a function of $t/t^*(\delta\varepsilon)$ showing that the results for different ε can be collapsed onto a single scaling function with two branches. The results for different ε correspond to different symbols. The inset shows the scaling parameter t^* as a function of ε/W for the upper (squares) and bottom (circles) branches. Other parameters as in Fig. 3.

the curve corresponding to $\varepsilon_i < U/2$ has $Z(t) = B^- t$, while that for $\varepsilon_i > U/2$ follows $1 - Z(t) = B^+ t$. These results are for a flat cavity field but, as mentioned earlier, we checked that the same exponents are found also for other bath functions, meaning that they are independent of the exact form of the cavity field.

The power-law behavior and the respective exponents observed numerically in the three limits above are con-

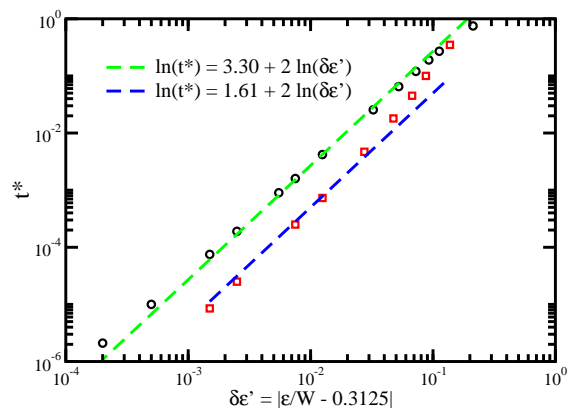


FIG. 6: (Color online) Scaling parameter t^* as a function of $\delta\varepsilon$ for the scaling procedure presented in Fig. 5. The results for the upper ($Z \rightarrow 1$) and the bottom ($Z \rightarrow 0$) branches correspond to squares and circles, respectively. For both branches, t^* follows a powerlaw with exponent equal to 2.

firmed if we solve the SB equations analytically close to the transition ($t \rightarrow 0$). For small ε_i , we have that Z_i goes as

$$Z_i \approx \frac{64V^2}{U^2} t \left(1 + \frac{8}{U^2} \varepsilon_i^2 \right), \quad (8)$$

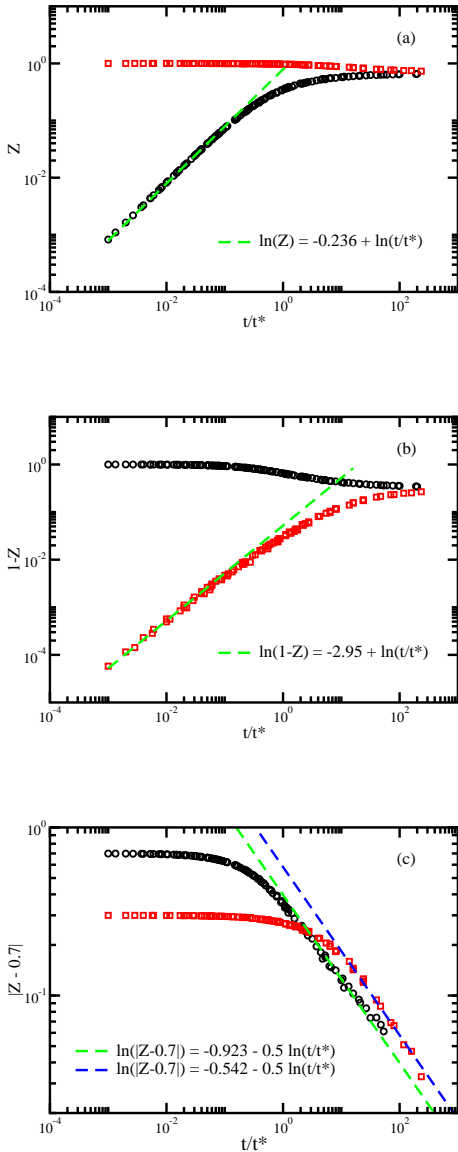


FIG. 7: (Color online) Same numerical data presented in Fig. 5 now showing the powerlaw behavior in three different cases: (a) $Z(t) \sim t$ for the sites with $\varepsilon < U/2$ (bottom branch) in the limit $t \rightarrow 0$, (b) $Z(t) \sim 1 - B^+ t$ for the sites with $\varepsilon > U/2$ (upper branch) in the limit $t \rightarrow 0$ and (c) $|Z(t) - Z^*| \sim A^\pm t^{-1/2}$ for the two branches when $t \gg 1$. In all panels, squares and circles correspond to the upper and the bottom branches, respectively.

that is, has a linear dependence on t , which corresponds to the same exponent obtained in the fitting shown in Fig. 7(a). In the opposite limit of large ε_i (more specifically, $\varepsilon_i \gg U/2$ and $\hat{\varepsilon}_i^2 \gg t$), in accordance with what is seen in Fig. 7(b), Z_i differs from 1 by a term which is linear in t ,

$$1 - Z_i \approx 3 \times 10^{-6} \frac{V^2}{\varepsilon_i^2} t. \quad (9)$$

Finally, for ε_i around and close to $\varepsilon^* = U/2$, we have

$$Z_i \approx \frac{2}{3} + \frac{1}{9V} \sqrt{\frac{2}{t}} (\varepsilon_i - U/2), \quad (10)$$

once more confirming the exponent equal to -0.5 seen in the numerical results of Fig. 7(c).

The results in eqs. (8-10) are valid for a simple flat bath. In case of a more general form for $\rho_{typ}(\omega)$, assuming $t \rightarrow 0$, the following substitution should be made in the above equations

$$t \rightarrow \int_{-t/2}^{t/2} d\omega \rho_{typ}(\omega). \quad (11)$$

Considering that the scaling properties shown in Fig. 2(b) hold, that is,

$$\rho_{typ}(\omega)/\rho_{typ}(0) = g(\omega/t), \quad (12)$$

where $g(y = \omega/t)$ is the scaling function, we can rewrite Eq. (11) as

$$t \rightarrow t \left[\rho_{typ}(0) \int_{-1/2}^{1/2} dy g(y) \right] \sim t. \quad (13)$$

This means that the same exponents for the power-law behavior in t are found independent of the specific form of the cavity field, as pointed out before.

In the following, we rationalize these findings by defining an appropriate β -function which describes all the fixed points and the corresponding crossover behavior. Let us assume that

$$\frac{dZ(t, \delta\varepsilon)}{d \ln t} = -\beta(Z) \quad (14)$$

is an explicit function of Z only, but not of the parameters t or $\delta\varepsilon$. The desired structure of the flows would be obtained if the β -function had three zeros: at $Z = 0$ and $Z = 1$ with negative slope (stable fixed points) and one at $Z = Z^*$ with positive slope (unstable fixed point).

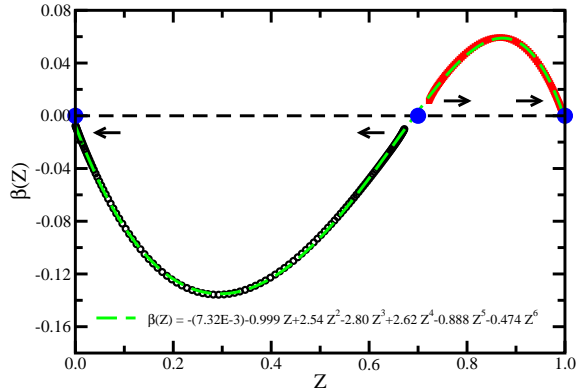


FIG. 8: (Color online) β -function obtained as described in the text for the Anderson impurity models close to the Mott-Anderson transition. The filled circles indicate the three fixed points found for this problem. The arrows indicate how Z flows to the stable points ($Z = 0$ and $Z = 1$) and from the unstable one ($Z \approx 0.7$).

A. How to determine the β -function?

Assuming that the general structure of these flows can be described in a β -function language similar to that used in the context of a renormalization group approach, we outline the procedure to obtain $\beta(Z)$ from the numerical data.

The integration of Eq. (14) can be written in the form of Eq. (7) as

$$Z = f[t/t^*(Z_o)], \quad (15)$$

where Z_o is the initial condition (a function of $\delta\varepsilon$). With $x = t/t^*$ as before, Eq. (7) can be rewritten as

$$\beta(Z) = -x f'(x). \quad (16)$$

The numerical data for $Z = f(x)$ as a function of x is presented in Fig. 5. It is possible to fit the two branches in this figure with simple functions, as the results in Fig. 7 suggest. Thus, using eq. (16), the β -function in terms of $x(Z)$ is determined, which can finally be rewritten in terms of Z . Carrying out this procedure, we obtain $\beta(Z)$ as shown in Fig. 8. In accordance with what was discussed above, we see that $\beta(Z)$ has three fixed points, as indicated in the figure by filled circles. $Z = 0$ and $Z = 1$ are stable, while $Z \approx 0.7$ is the unstable fixed point.

This procedure proves that a β -function formulation is valid in the case of the Anderson impurity models when approaching the Mott-Anderson transition. The scaling behavior and the associated β -function observed here reflect the fact these impurity models have two phases (singlet and doublet) when entering the insulator. The two stable fixed points describe these two phases, while the unstable fixed point Z^* describes the phase transition, which is reached by tuning the site energy. To completely solve the problem of the Mott-Anderson transition, however, the bath function “seen” by the *ensemble* of single-impurity problems has to be self-consistently determined. The results obtained in this case are left to be discussed elsewhere.¹⁵

IV. CONCLUSIONS

In this paper, we focused on understanding the behavior of Anderson impurity problems in a model bath chosen to mimic the approach to the Mott-Anderson transition. We presented numerical and analytical results that portray a simple scaling behavior in the critical regime where the bath spectral weight becomes vanishingly small. Our scaling analysis clarifies the emergence of the two-fluid behavior at the critical point, which can be considered as a first step towards constructing a full self-consistent description of the Mott-Anderson transition.

The scaling behavior and the associated β -function observed by us reflect the fact that, when entering the insulator, the impurity models have two phases (singlet and doublet), undergoing a phase transition as the site energy is tuned. In this sense, most of our conclusions represent properties of the Anderson impurity models in the relevant strong-coupling limit, and as such have a potential use beyond the possible application to a specific self-consistent scheme such as the TMT approach.¹² Indeed, we expect that similar critical scaling properties apply in a more sophisticated *statDMFT* theory,¹¹ where the impurity is embedded in a statistical *ensemble* of fluctuating baths. Applied to this problem, the present work opens an avenue to analytically characterize the scaling of the relevant distribution functions in the critical regime.

Incorporating what we learned about the impurity models into these self-consistent schemes is an interesting and important problem left for future work.

This work was supported by NSF grants DMR-0234215 (VD) and DMR-0528969 (GK). MCOA was supported in part by NSF grant DMR-0312495.

¹ N.F. Mott, *Metal-insulator Transitions* (Taylor and Francis, London, 1974).

² P.W. Anderson, Phys. Rev. **109**, 1498 (1958).

³ E. Abrahams, P.W. Anderson, D.C. Licciardello and T.V. Ramakrishnan, Phys. Rev. Lett. **42**, 673 (1979).

⁴ A.M. Finkelstein, Z. Phys. B - Condensed Matter **56**, 189

- (1984).
- ⁵ A. Gold and V.T. Dolgoplov, *Phys. Rev. B* **33**, 1076 (1986).
- ⁶ S. Das Sarma and E.H. Hwang, *Phys. Rev. Lett.* **83**, 164 (1999).
- ⁷ G. Zala, B.N. Narozhny and I.L. Aleiner, *Phys. Rev. B* **64**, 214204 (2001).
- ⁸ A. Punnoose and A.M. Finkel'stein, *Science* **310**, 289 (2005).
- ⁹ For reviews, see P.A. Lee and T.V. Ramakrishnan, *Rev. Mod. Phys.* **57**, 287 (1985); D. Belitz and T.R. Kirkpatrick, *Rev. Mod. Phys.* **66**, 261 (1994).
- ¹⁰ A. Georges, G. Kotliar, W. Krauth, and M.J. Rozenberg, *Rev. Mod. Phys.* **68**, 13 (1996).
- ¹¹ V. Dobrosavljević and G. Kotliar, *Phys. Rev. Lett.* **78**, 3943 (1997).
- ¹² V. Dobrosavljević, A.A. Pastor, and B.K. Nikolić, *Europhys. Lett.* **62**, 76 (2003).
- ¹³ K. Byczuk, W. Hofstetter, and D. Vollhardt, *Phys. Rev. Lett.* **94**, 056404 (2005).
- ¹⁴ G. Kotliar and A.E. Ruckenstein, *Phys. Rev. Lett.* **57**, 1362 (1986). The method was applied in the disorder problem by D. Tanasković, V. Dobrosavljević, E. Abrahams, and G. Kotliar, *Phys. Rev. Lett.* **91**, 066603 (2003).
- ¹⁵ M.C.O. Aguiar, V. Dobrosavljević, E. Abrahams, and G. Kotliar, to be published.
- ¹⁶ Within TMT, the typical DOS represents the extended states of the system and as such has its spectral weight going to zero as the Mott-Anderson is approached. The (arithmetic) average DOS includes both extended and localized states and it is its spectral weight that is normalized within this method.